

Article

Not peer-reviewed version

Finite Element Analysis of Functionally Loaded Subperiosteal Implants Evaluated on a Realistic Model Reproducing Severe Atrophic Jaws

[Gerardo Pellegrino](#) , [Maryia Karaban](#) ^{*} , Veronica Scalchi , Marco Urbani , [Amerigo Giudice](#) , [Carlo Barausse](#) , [Pietro Felice](#)

Posted Date: 5 December 2024

doi: 10.20944/preprints202412.0504.v1

Keywords: [juxta-osseous implants](#); [severe jaw atrophy](#); [Finite Element Analysis \(FEA\)](#)



Preprints.org is a free multidisciplinary platform providing preprint service that is dedicated to making early versions of research outputs permanently available and citable. Preprints posted at Preprints.org appear in Web of Science, Crossref, Google Scholar, Scilit, Europe PMC.

Copyright: This open access article is published under a Creative Commons CC BY 4.0 license, which permit the free download, distribution, and reuse, provided that the author and preprint are cited in any reuse.

Disclaimer/Publisher's Note: The statements, opinions, and data contained in all publications are solely those of the individual author(s) and contributor(s) and not of MDPI and/or the editor(s). MDPI and/or the editor(s) disclaim responsibility for any injury to people or property resulting from any ideas, methods, instructions, or products referred to in the content.

Protocol

Finite Element Analysis of Functionally Loaded Subperiosteal Implants Evaluated on A Realistic Model Reproducing Severe Atrophic Jaws

Gerardo Pellegrino ¹, Maryia Karaban ^{2,*}, Veronica Scalchi ³, Marco Urbani ⁴, Amerigo Giudice ⁵, Carlo Barausse ⁶ and Pietro Felice

¹ Department of Biomedical and Neuromotor Sciences, University of Bologna, Bologna, Italy

² Department of Biomedical and Neuromotor Sciences, University of Bologna, Bologna, Italy

³ 3D product specialist, custom made medical devices, BTK Dental, Italy

⁴ 3D product specialist, custom made medical devices, BTK Dental, Italy

⁵ Department of Health Sciences of the 'Magna Graecia' University of Catanzaro, Italy

⁶ Department of Biomedical and Neuromotor Sciences, University of Bologna, Bologna, Italy

⁷ Department of Biomedical and Neuromotor Sciences, University of Bologna, Bologna, Italy

* Correspondence: maryia.karaban2@unibo.it

Abstract: Implant-supported prosthetic rehabilitation for patients with severely atrophic jaws is challenging due to complex anatomical considerations and the limitations of conventional augmentation techniques. This study explores the potential of subperiosteal (juxta-osseous) implants as an alternative solution, using finite element analysis (FEA) to evaluate mechanical performance. Realistic jaw models, developed from radiographic data, are utilized to simulate various implant configurations and load scenarios. Results indicate that different screw placements, implant designs, and structural modifications can significantly influence stress distribution and biomechanical behavior. Upper and lower jaw models were assessed under multiple load conditions to determine optimal configurations. Findings suggest that strategic adjustments, such as adding posterior screws or altering implant connections, can enhance load distribution and reduce stress concentration, particularly in critical areas. The study provides evidence-based insights into optimizing subperiosteal implant design to improve stability, longevity, and patient outcomes.

Keywords: juxta-osseous implants; severe jaw atrophy; Finite Element Analysis (FEA)

1. Introduction

It is widely recognized that implant-supported fixed prosthetic rehabilitation for patients with severely atrophic jaws poses significant challenges for clinicians [1]. Current surgical options for bone augmentation and subsequent standard-length implant placement include inlay/onlay bone grafting, guided bone regeneration (GBR) with resorbable or non-resorbable membranes, and distraction osteogenesis. However, these methods typically require multiple surgeries, which can lead to postoperative morbidity, graft failure, prolonged treatment timelines, and significant costs [2, 3].

As an alternative to the bone augmentation procedures, reduced-length or reduced-diameter implants can be considered. While short and ultrashort implants are viable options, they necessitate a minimum of 6 mm of bone height above the mandibular canal and at least 4 mm of bone height below the maxillary to host the shortest implants available [4, 5]. Additionally, a minimum of 5 mm of crestal residual width is needed to place 3 mm diameter implants. In cases of extreme jaw atrophy, meeting these conditions may be impossible due to the proximity of critical anatomical structures, making the placement of short, ultrashort, and narrow implants challenging or even impossible [6].

Another potential solution is the use of tilted implants, which involves positioning standard implants in less resorbed areas of the jaw and angling them distally or mesially to achieve prosthetic rehabilitation of the adjacent site as well. However, tilted implants may be at risk of biomechanical failure, and the angulation is always dependent on the type of abutment used [7, 8].

Zygomatic and pterygoid implants aim to circumvent the need for bone regeneration augmentation but present their own set of challenges. These procedures carry inherent risks of intra- and post-operative complications, are associated with high costs, and require the expertise of a highly experienced surgeon [9].

In addition to the latest advancements in biomedical technology, such as of Computer-aided design (CAD) /Computer-aided manufacturing (CAM) and personalized medicine, new trends in personalized medicine, including laser melting techniques, are emerging [10-13].

In contrast to traditional methods, subperiosteal implants, also known as juxta-osseous implants, offer an alternative for implant-supported prosthetic rehabilitation. These implants are typically made of titanium and feature a three-dimensional design with a basal frame and wings that include holes for cortical bone fixation using screws [14]. Subperiosteal implants are placed directly on the jawbone and covered with periosteum, with transmucosal tunnel connections. The structure can be configured into separate right and left components or interconnected with an intraoral connector, depending on the residual anatomy of the jaw [15].

Despite several studies and scientific literature, there are currently no standardized protocols defining the criteria for designing these implants to minimize stress on the structure and reduce impact on the patient's bone [16]. The number and positioning of screws, among other factors, can influence the success of the treatment. To evaluate these parameters clinically, a significant number of patients would be needed for reliable results. In industrial settings, biomechanical feedback can help address this issue by assessing the design and positioning of screws. This approach involves biomechanical feedback related to the structural design and configuration of the implants.

Therefore, the aim of this study is to conduct mechanical and stress evaluations using finite element analysis (FEA) on anatomically accurate jaw models of patients. FEA is crucial for simulating and assessing mechanical performance, helping to optimize implant design for enhanced stability, longevity, and patient comfort [17]. To achieve these results, realistic models must be prepared to obtain biomechanical feedback, including cortical and medullary bone thickness and elastic modulus [18].

This approach not only facilitates theoretical predictions but also informs clinical decision-making by providing evidence-based insights into the biomechanical behavior of subperiosteal implants in real-world applications. The object of the study is to evaluate differences in implant configuration, considering screw positioning and number, extension, design, and stress under various axial and non-axial loads, both in the anterior and posterior regions. It will also assess the biomechanical response of realistic bone models.

2. Materials and Methods

A case involving extreme mandible and maxilla was selected, both presenting typical characteristics, thereby excluding extreme cases of bone atrophy [19]. The Digital Imaging and Communications in Medicine (DICOM) files, obtained from the radiographic examination, were segmented to isolate only the bone volume with the help of the RealGuide - 3Diemme software. Surface tessellation language (STL) of the portion of the skull below the eye sockets (upper part) and of the entire mandible (lower part) were obtained. The surfaces and volumes extrapolated from the radiographic examination were subjected to processing, in order to repair small defects and to simplify the geometry. These operations were performed using Meshmixer software. Through the same software it was also possible to recreate the cancellous bone volume where present, as the border between cortical and spongy bone is not always clear after the direct export of this volume starting from the radiographic examination. Cortical bone thickness measurements were therefore performed in various areas of the model, the cancellous bone volume was obtained by offset with respect to the previously extracted bone surfaces.

Following the standard design process, the juxta-osseous implant was modeled onto the previously processed STL files. A preliminary draft of the prosthetic structure was also developed to position the abutments accurately and to identify the points of application for masticatory loads. Using reverse engineering software Cyborg3D, parametric surfaces were reconstructed from the STL

files, which are more compatible with current software. The files for the mandible, maxilla, and juxta-osseous implant were then converted to STEP format. Using SolidEdge CAD software, additional details were added to the model, such as the cortical fixation screws. These screws were modeled in a simplified manner as excessive detail in the geometry would have led to excessively long computation times and overly complex results for the purpose of the analysis. The next phase of the study focused on defining contact properties between different components of the system. Two types of contact were established: glued contact, permanently bonds surfaces as if glued together, preventing detachment or sliding, and frictional contact, allows surfaces to slide and detach from each other.

Specific surfaces within the geometric model were identified and paired using connectors, each assigned one of these contact properties:

- Between bone support and juxta support surfaces: Frictional contact simulates realistic interaction.
- Between cortical bone and spongy bone surfaces: Glued contact simulates their natural bond.
- Between screw threads and bone surfaces: Simplified with glued contact due to screw geometry and assumed osseointegration.
- Between screw underhead and juxta seats: Contact type property allows small displacements.
- Between juxta abutments and prosthesis: Glued contact solidifies the implant-to-prosthesis connection.

Initial settings ensured zero penetration or gap, eliminating minor geometric imperfections. Materials were defined as isotropic and linear, with average bone characteristics adopted. Meshing employed tetragonal elements adaptable to varying geometries. For the characterization of the bone, average values were adopted since the properties vary depending on numerous parameters such as age, physiology, and pathologies of the patient.

Mesh creation proceeded using tetrahedral elements for all geometries of the model. The element sizes set were as follows: 1.5 mm for the general cortical bone, 1 mm for implant support areas, and 0.5 mm for cortical screw holes. For the spongy bone, element sizes were 1.5 mm for general areas and 1 mm for cortical screw holes. Juxta-osseous implants were meshed with 0.7 mm elements in general areas and 0.5 mm at cortical screw sites. Cortical screws were meshed with 0.5 mm elements. The prosthesis was meshed with 1.5 mm elements. These element sizes were chosen to ensure an accurate representation of the various geometries and areas of interest in the FEA model.

The term σ_{max} allowable refers to the maximum stress that the material can withstand. In the case of titanium, this corresponds to the yield strength, while in the case of bone, it is a value derived from the literature and represents a safety load sufficient to prevent resorption effects. Loads were applied through node displacements in five configurations, each analyzed to assess structural responses under different load placements. All loads were vertically oriented, reflecting masticatory loads of 500N. A stress limit of 50 MPa on bone was identified to prevent resorption effects (Table 1).

Table 1. The characteristics of the material and the mesh adopted from the literature.

Type of material	Elastic module E (MPa)	Poisson coefficient	σ_{max} Maximum allowable (Mpa)
Cortical bone	13700	0.3	50
Trabecular bone	1370	0.3	-
Titanium Gr5 (load model)	101000	0.34	950
Titanium Gr5 (bar)	101000	0.34	970
Resin for prosthetics	3000	0.3	-
Muscle simulators	25	0.4	-

The loads were applied by imposing displacements at specific nodes of the model. Specifically, displacements were applied in 5 different configurations, each of which was analyzed individually to assess how the structure responded based on the point of load application.

3. Results

As mentioned above, various load configurations were adopted. In the analysis of the first model (V0), the configuration that generated the highest stresses in the system was identified. All subsequent models were computed for all load configurations, but the optimization of the geometry was developed based on the most severe condition. The stresses are indicated in MPa.

Upper jaw models:

- Model V0. From the analysis of Model V0, it emerged that the most critical situation is related to load configuration 3 (Figure 1a, b), which represents a load applied to the anterior right side. The least critical situations are load configurations 1 and 2 (Figures 2 and 3), corresponding to a load distributed across the entire dentition and a load distributed only on the posterior teeth, respectively. Regarding the stress values observed, no critical issues were identified with the juxta-osseous implant. In load configuration 3, the stresses are below the breaking limits of titanium laser melting: peak stresses of 500 MPa are reached only in very localized areas of the implant.
- Model V1. Added posterior screws, reducing stress on anterior parts and achieving more balanced distribution. The addition of the posterior screw has certainly alleviated the load on the palatal screw, which was excessively stressed in the previous model (Figure 4). The screw now experiencing the most stress is the posterior screw: compared to the previous case, only part of the hole shows a stress exceeding 50 MPa, and the area affected by this stress is therefore much more contained (Figure 5a, b).
- Model V2. This model serves as an alternative to model V1, as it aims to stabilize the structure posteriorly using screws placed in the vestibular direction rather than the palatal direction (Figure 6). Similar behavior to V1, leading to the decision to proceed with V1 for further development (Figure 7).
- Model V3. Based on the findings from model 1, attention was shifted to the anterior section to optimize the anchors in that area. Two additional screws were placed anterior to the nasal spine to reduce the load on the frontal screws (Figure 8). The analysis revealed minimal changes; the stress on the frontal screws remains the same, while the pressure on the anterior crestal support has decreased to below 35-40 MPa (Figure 9).
- Model V4. The previously added screw was relocated towards the frontal process, aligning it vertically with the other screws and ensuring that both arms of the first and second abutments connect to this screw (Figure 10). This solution proved to be more effective than V3; the addition of the screw reduces the stress on the other screws and on the support. The area where stress exceeds 50 MPa in the vicinity of the screws is now more contained, and the crestal support shows stresses between 30 and 35 MPa, which are absolutely acceptable (Figure 11).
- Model V5. This model determined whether the connection between the two hemi-implants affects the behavior and stability of the implant. Specifically, in this model, a frontal connecting bar was added while the palatal bar was removed (Figures 12 and 13).
- Model V6. This model analyzes an implant divided into two hemi-arches without any connecting element. As can be easily observed, the presence or absence of an element joining the two halves of the implant has no effect on the stress state of the model. In all previously analyzed models, the bar connecting the two hemi-arches of the implant shows no stress (Figure 14). Removing this bar in model 6 does not alter the results in any way; the stress state of the bone and implant remains the same as in cases with the connection (Figure 15).

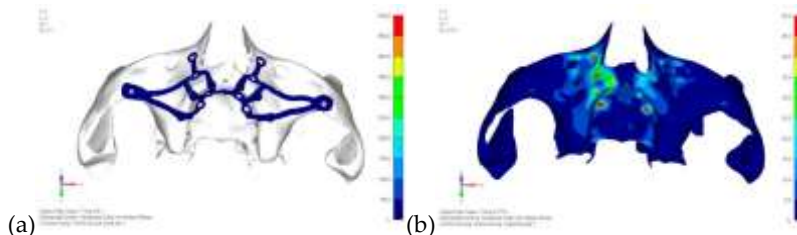


Figure 1. (a) Design of the subperiosteal implant on the upper jaw model V0; (b) Model V0 with the most critical anterior right side load configuration 3.



Figure 2. Model V0 with the least critical load configuration 1 distributed across the entire dentition.



Figure 3. Model V0 with the least critical load configuration 2 distributed across the posterior teeth.

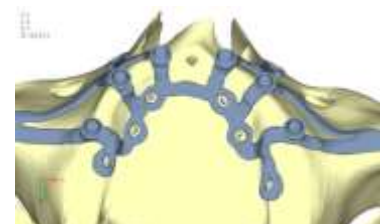


Figure 4. Design of the subperiosteal implant on the upper jaw model V1 with added posterior screws, reducing stress on anterior parts and achieving more balanced distribution.

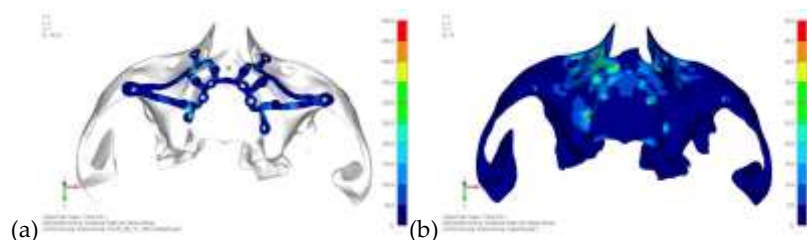


Figure 5. (a) Design of the subperiosteal implant on the upper jaw model V1; (b) Upper jaw model V1 with added posterior screws, reducing stress on anterior parts and achieving more balanced distribution.

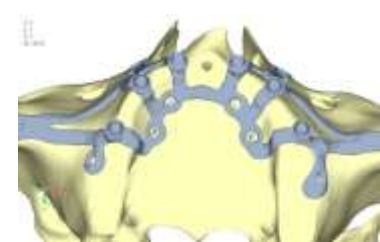


Figure 6. Design of the upper jaw model V2 structure using screws placed posteriorly in the vestibular direction rather than the palatal direction.

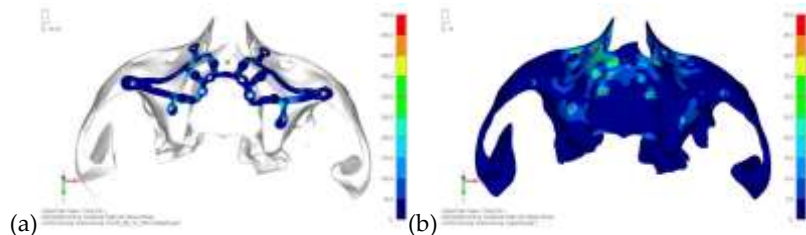


Figure 7. (a) Design of the subperiosteal implant on the upper jaw model V2; (b) Loading distribution across the upper jaw model V2, similar behavior to the model V1.



Figure 8. Design of the upper jaw model V3 using screws placed in the vestibular direction rather than the palatal direction.

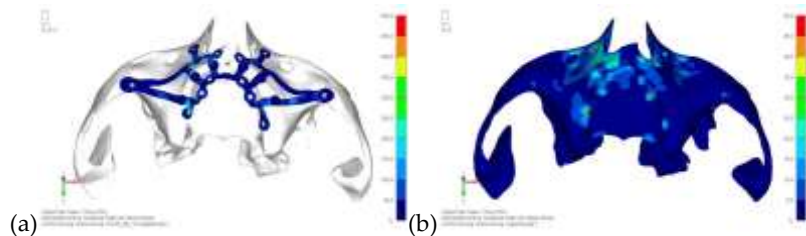


Figure 9. (a) Design of the subperiosteal implant on the upper jaw model V3; (b) Upper jaw model V3 with optimized front section with additional screws, stress on frontal screws remained unchanged.



Figure 10. Design of the upper jaw model V4 with the added screws relocated towards the frontal process, aligning them vertically with the other screws and ensuring that both arms of the first and second abutments connect to this screw.

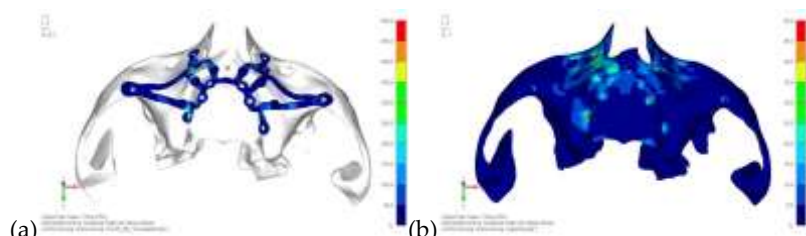


Figure 11. (a) Design of the subperiosteal implant on the upper model V4; (b) Stress loading on the upper model V4 exceeds 50 MPa in the vicinity of the screws, but is now more contained. The crestal support shows stresses between 30 and 35 MPa.

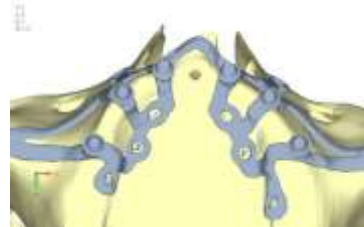


Figure 12. Design of the model V5 with the connection between the two hemi-implants, affecting the structure. A frontal connecting bar was added while the palatal bar was removed.

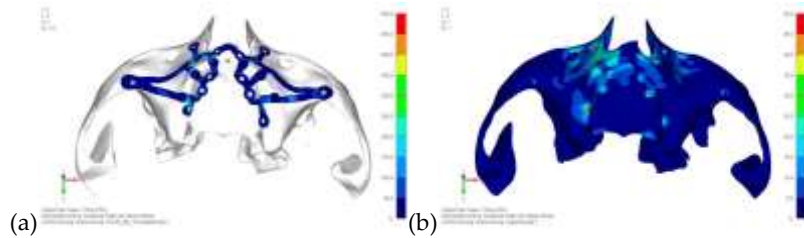


Figure 13. (a) Design of the upper jaw model V5; (b) Stress loading on the model V5 with the frontal connecting bar.

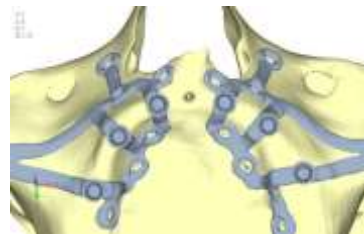


Figure 14. Design of the model V6 divided into two hemi-arches without any connecting element.

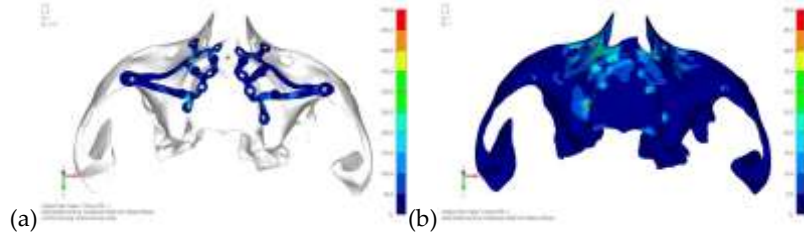


Figure 15. (a) Design of the upper jaw model V5; (b) Stress loading on the model V6 of the bone and implant remains the same as in cases with the connection.

This effect is clearly due to the presence of the prosthesis, which is not visualized in the model but is included in the numerical calculations. The prosthesis helps to stiffen the system without the need for a connecting element at the implant level. As can be easily observed, the presence or absence of an element joining the two halves of the implant has no influence on the stress state of the model. In all previously analyzed models, the bar connecting the two hemi-arches of the implant shows no stress. Removing this bar in Model 6 does not alter the results in any way; the stress state of the bone and implant remains the same as in cases with the connection.

Lower jaw models:

The same approach as the upper jaw was adopted, the model was analyzed in different load configurations to identify the most onerous situation.

- Model V0. This model represents the initial analysis performed on the lower arch. The implant consists of two completely separate hemi-arches. The situation observed in the lower model is very similar to that found in the upper model. The most significant load is load 3 (Figure 16), corresponding to chewing in the anterior right sector. Loads distributed over larger areas,

such as configurations 1 and 2, result in less stress on both the implant and the bone (Figure 17 and 18).

- Even in the lower model, the stresses observed in the peri-implant bone are always acceptable and significantly lower compared to those found in the upper implant. In the worst case, peak stresses reached 250 MPa, which ensures an adequate safety margin. From the bone perspective, in load configuration 3, it is noted that stresses exceed 50 MPa even in areas distant from the implant, such as near the condyles and in the posterior alveolar process.
- Model V1. In this version of the implant, two anterior appendages have been added in a crestal position with the aim of better distributing the load in that area (Figure 19). The examined configuration masnot result in improvements. Additionally, from a practical standpoint, it is unfeasible because the presence of the crestal screws would create an obstacle in managing the soft tissues, increasing the risk of dehiscence and exposure of the implant (Figures 20 and 21).
- Model V2. The implant has been modified anteriorly by extending the anterior vestibular arms that connect to the first abutment (Figure 21). This change aims to achieve greater flexibility of the implant in that area, promoting the transmission of masticatory load to the bone through support rather than through the screws. The modification did not reveal significant changes in the stress state. The stresses near the holes are similar to those observed in Model 1 (Figure 22).
- Model V3. To reduce the load on the front screws, it was decided to add an additional screw, distributing the load of the anterior abutment across 3 screws instead of 2 (Figure 23). The addition of the anterior screw has certainly improved the distribution of stresses, as the volume of material experiencing stresses greater than 50 MPa near the screws has decreased (Figure 24).
- Model V4. This version was derived from Version 3 by adding a screw in the posterior sector, positioned in the vestibular direction (Figure 25). Again, the addition of an anchoring screw has allowed for more effective distribution of the stresses. The posterior alveolar area, particularly around the more posterior screws, remains notably stressed (Figure 26). However, this phenomenon is attributed to the geometry and configuration of the bone rather than the presence of a cortical screw.
- Model V5. This version of the implant retains the same geometry as Version 4, with the addition of two connecting bars, one on the lingual side and one on the vestibular side (Figure 27). The purpose of this analysis is to identify the differences between a monolithic implant and an implant divided into two hemi-arches. The results are quite similar to those observed in the upper model: the presence of a connection between the two halves of the implant does not contribute to its stability. It is immediately noticeable that the two connecting bars exhibit stresses close to 0, indicating that no force is transmitted through them (Figure 28). Once again, a significant contribution is provided by the prosthesis, which stiffens the structure through the abutments.

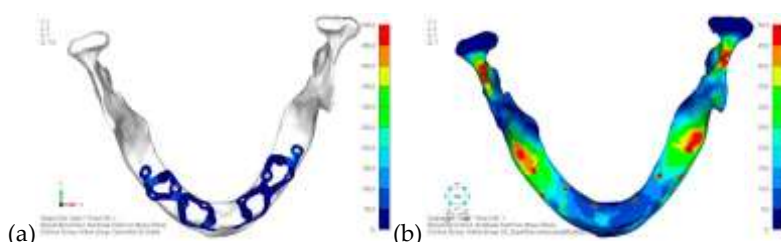


Figure 16. (a) Design of the subperiosteal implant on the lower jaw model V0; (b) The most significant load on the lower jaw model V0, corresponding to chewing in the anterior right sector.

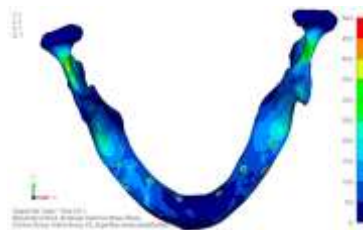


Figure 17. Load configuration 1 distributed over a larger area of the lower jaw model V0.

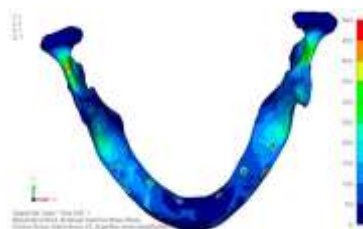


Figure 18. Load configuration 2 distributed over a larger area of the lower jaw model V0.



Figure 19. Design of the model V1 with two anterior appendages added in a crestal position.

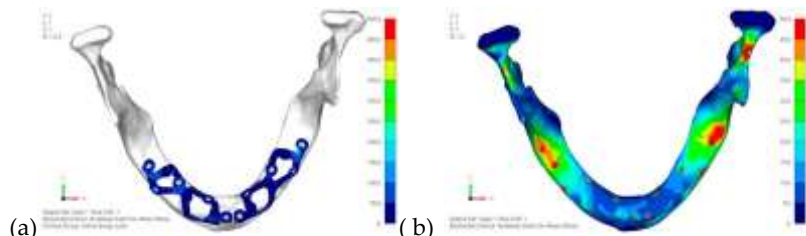


Figure 20. (a) Design of the subperiosteal implant on the lower jaw model V1; (b) Stress loading on the model V1 and implant, with no improvement in the configuration observed.

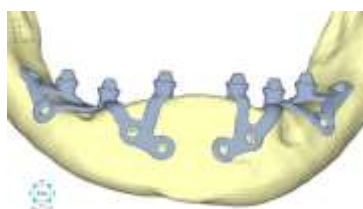


Figure 21. Design of the model V2 with extended anterior vestibular arms that connect to the first abutment.

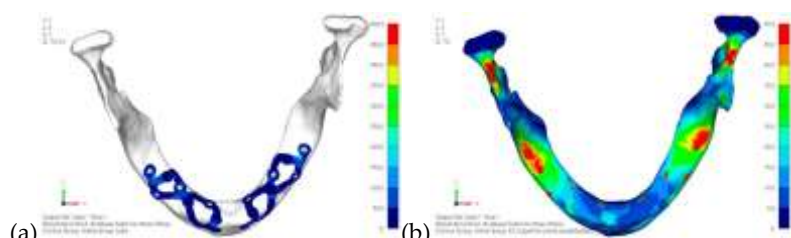


Figure 22. (a) Design of the subperiosteal implant on the lower jaw model V2; (b) The stresses near the holes in the model V2 are similar to those observed in model V1.



Figure 23. Model V3 design with an additional screw, distributing the load of the anterior abutment across 3 screws instead of 2.

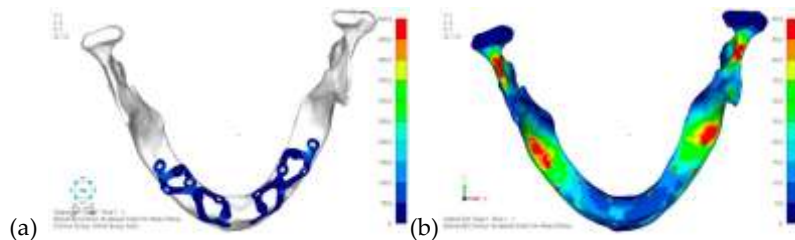


Figure 24. (a) Design of the subperiosteal implant on the lower jaw model V3; (b) Decreased stress loading on the material of the model V3.



Figure 25. Model V4 design 3 by adding a screw in the posterior sector, positioned in the vestibular direction to the model V3.

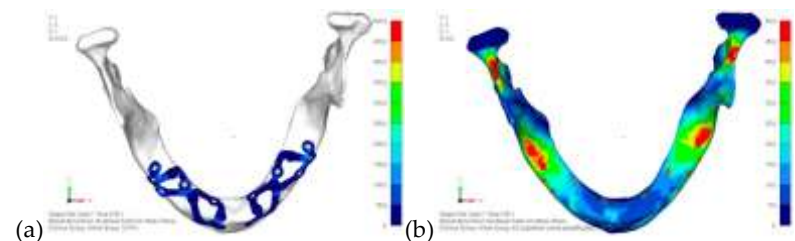


Figure 26. (a) Design of the subperiosteal implant on the lower jaw model V4; (b) The posterior alveolar area of the model V4, particularly around the more posterior screws, remains notably stressed.



Figure 27. Model V5 design with the same geometry as version 4, with the addition of two connecting bars, one on the lingual side and one on the vestibular side.

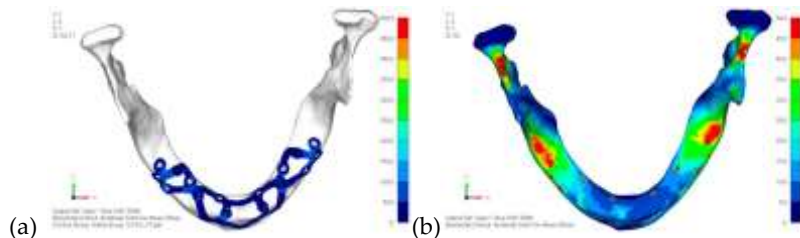


Figure 28. (a) Design of the subperiosteal implant on the lower jaw model V5; (b) Stress loading on the model V5 on the two connecting bars exhibits stresses close to 0, indicating that no force is transmitted through them.

4. Discussion

The present study aimed to simulate on a realistic anatomical model the design of juxta-osseous implants in order to evaluate the biomechanical stress on the implant and the bone. One case concerning the mandible and the maxilla were selected for the study, presenting typical characteristics of severe bone atrophy [19], for which designing juxta-osseous implants for the future prosthetic rehabilitation could be a valid treatment option. A similar study was conducted by De Moore 2022, analyzing even more extreme cases of bone atrophy, and the design of subperiosteal implants was found to be completely safe and considered a great solution for implant-supported fixed rehabilitation [20].

For the recent study, various load simulations and designs of juxta-osseous implants were analyzed. The structural tension values were extrapolated from the literature, representing an average load [21]. The recent study of Ayhan 2023, showed that 1 mm thick implants show more displacement than 1.5 mm thick ones, even though the differences between the groups are negligible [22]. However, the analyses of the present study have highlighted that the metal structure of the subperiosteal implant effectively withstands masticatory loads, with no particular issues in terms of stresses. Therefore, the thicknesses of the metall structure adopted for the design (0.7 mm in the general area and 0.5 mm) was suitable for the purpose.

Studying different types of loading Antiparmak (2023) revealed that the cortical bone experienced the highest minimum principal stress values under posterior oblique loading forces [23]. Meanwhile, Zielinski's research (2023) highlighted that while vertical loads at 90 degrees induced minimal strain and stress, non-axial forces significantly escalated stress levels in multi-unit configurations, reaching nearly 500 MPa [24]. The present study focused on vertical forces without analyzing any oblique forces, which may limit its scope. Further investigation into the effects of oblique forces is warranted to provide a more comprehensive understanding of the topic. The results of the present study indicated that the most significant load occurred during the anterior load, aligning these data with the recently published studies [23-25]. Larger load distributions, as seen in configurations 1 and 2, resulted in reduced stresses on both the implant and bone. Critical areas in the bone, especially near cortical fixing screws, experienced tensile loads exceeding 50 MPa. The constant load applied across all dentition areas contributed to the stress distribution observed. It is preferable to have a lower masticatory force on the anterior sectors compared to the posterior ones.

The most stressed screw sites were the posterior and anterior vestibular ones. The presence of crestal screws was minimized to avoid clinical issues related to soft tissue management and reduce the risk of dehiscence and implant exposure. It is important to note that in Ayhan's study, there is a specific emphasis on screw use being a more critical factor affecting bone stress than implant design. This underscores the importance of carefully evaluating screw positioning during surgical procedures [22].

The fixation of the implants in the anterior and posterior sectors was crucial: in the posterior area, the last screw was retracted as much as possible to increase the force generated by the screw. In the anterior sector, having a sufficient number of screws in the buccal direction is essential to support the shear loads. In the upper case, three screws were arranged, aligning them approximately vertically and laterally to the nasal cavity. In the lower model, the adequate number of screws was found to be three, which support the first and second abutments [24].

Although, Ayhan 2023 study revealed that dual implants demonstrated lower von Mises stress within the implant structure compared to mono implants. Mono implants exerted less force on the bone, leading to a more uniform load distribution across the upper jaw and consequently lower residual stresses in the bone [22]. There is no difference in present study in bone tension and the structure's tension between one-piece and two-piece implants. This effect is could be due to the presence of the prosthesis, which helps to stiffen the system without requiring a connecting element at the implant level. It is worth noting that the material constituting the prosthesis in these models is dental engineering resin; if the prosthesis were made of a metallic material, it could further stiffen the implant-prosthesis system.

5. Conclusions

The present study highlighted the biomechanical characteristics of iuxta-osseous implant under masticatory load. For both the upper and lower models, the heaviest load configuration was found to be the one with the load applied at the front. The analyses indicated that the metal structure of the juxta-osseous implant effectively withstands masticatory loads, with no critical issues regarding tension being identified. However, the proper fixation of the implants was crucial. No significant differences were observed between a one-piece implant and an implant divided into two parts in either model. The role of the prosthesis, which reinforces and stiffens the structure, was found to be essential. Nevertheless, to validate the results of this study, clinical trials are required.

Author Contributions: Conceptualization, Gerardo Pellegrino and Maryia Karaban; methodology, Veronica Scalchi; formal analysis, Marco Urbani; data curation, Amerigo Giudice; writing—original draft preparation, Maryia Karaban and Carlo Barausse; writing—review and editing, Maryia Karaban and Pietro Felice. All authors have read and agreed to the published version of the manuscript.

Institutional Review Board Statement: Not applicable.

Data Availability Statement: The original contributions presented in this study are included in the article. Further inquiries can be directed to the corresponding author .

Conflicts of Interest: The authors declare no conflicts of interests.

References

1. Alotaibi, F.F.; Rocchietta, I.; Buti, J.; D'Aiuto, F. Comparative evidence of different surgical techniques for the management of vertical alveolar ridge defects in terms of complications and efficacy: A systematic review and network meta-analysis. *J. Clin. Periodontol.* 2023, **50**, 1487-1519.
2. Urban, I.A.; Montero, E.; Monje, A.; Sanz-Sánchez, I. Effectiveness of vertical ridge augmentation interventions: A systematic review and meta-analysis. *J. Clin. Periodontol.* 2019, **46** (Suppl. 21), 319-339.
3. Lizio, G.; Pellegrino, G.; Corinaldesi, G.; Ferri, A.; Marchetti, C.; Felice, P. Guided bone regeneration using titanium mesh to augment 3-dimensional alveolar defects prior to implant placement: A pilot study. *Clin. Oral Implants Res.* 2022, **33** (6), 607-621.
4. Barausse, C.; Ravidà, A.; Bonifazi, L.; Pistilli, R.; Saleh, M.H.A.; Gasparro, R.; et al. Extra-short (4-mm) implants placed after regenerative failures in the posterior atrophic mandible: A retrospective study. *Int. J. Oral Implantol. (Berl.)* 2023, **16** (1), 31-38.
5. Stacchi, C.; Rapari, A.; Lombardi, T.; Bernardello, F.; Nicolin, V.; Berton, F. Does new bone formation vary in different sites within the same maxillary sinus after lateral augmentation? A prospective histomorphometric study. *Clin. Oral Implants Res.* 2022, **33** (3), 322-332.
6. Felice, P.; Pistilli, R.; Zucchelli, G.; Simion, M.; Karaban, M.; Bonifazi, L.; et al. Decision criteria proposed for the treatment of vertical bone atrophies in the posterior mandible. *Int. J. Periodont Rest Dent.* 2021, **41**, 71-77.
7. Fabbro, M.; Bellini, C.M.; Romeo, D.; Francetti, L. Tilted implants for the rehabilitation of edentulous jaws: A systematic review. *Clin. Implant Dent. Relat. Res.* 2012, **14** (4), 612-621.
8. Pozzan, M.C.; Grande, F.; Mochi Zamperoli, E.; Tesini, F.; Carossa, M.; Catapano, S. Assessment of preload loss after cyclic loading in the OT Bridge System in an "All-on-Four" rehabilitation model in the absence of one and two prosthesis screws. *Materials (Basel)* 2022, **15** (4), 1582.
9. Gabriele, G.; Chisci, G.; Cascino, F.; Ricci, N.M.; Marruganti, C.; Ferrari, M. Technique-related survival rate and complications of zygomatic implant placement: A systematic review and meta-analysis. *Int. J. Maxillofac. Implants* 2023, **38** (5), 855-875.

10. Mello, C.C.; Lemos, C.A.A.; Gomes, J.M.D.L.; Verri, F.R.; Pellizzer, E.P. CAD/CAM vs conventional technique for fabrication of implant-supported frameworks: A systematic review and meta-analysis of in vitro studies. *Int. J. Prosthodont.* 2019, **32** (2), 182-192.
11. Ahmed, K.S.; Ibad, H.; Suchal, Z.A.; Gosain, A.K. Implementation of 3D printing and computer-aided design and manufacturing (CAD/CAM) in craniofacial reconstruction. *J. Craniofac. Surg.* 2022, **33** (6), 1714-1719.
12. Pellegrino, G.; Basile, F.; Relics, D.; Ferri, A.; Grande, F.; Tarsitano, A.; Marchetti, C. Computer-aided rehabilitation supported by zygomatic implants: A cohort study comparing atrophic with oncologic patients after five years of follow-up. *J. Clin. Med.* 2020, **9** (10), 3254.
13. Stefanelli, L.V.; Franchina, A.; Pranno, A.; Pellegrino, G.; Ferri, A.; Pranno, N.; et al. Use of intraoral scanners for full dental arches: Could different strategies or overlapping software affect accuracy? *Int. J. Environ. Res. Public Health* 2021, **18** (19), 9946.
14. El-Sawy, M.A.; Hegazy, S.A. Subperiosteal implants constructed with digital technology: A systematic review. *Oral Maxillofac. Surg.* 2024, April 20. [Epub ahead of print].
15. Strappa, E.M.; Memè, L.; Cerea, M.; Roy, M.; Bambini, F. Custom-made additively manufactured subperiosteal implant. *Minerva Dent. Oral Sci.* 2022, **71** (6), 353-360.
16. Anitua, E.; Eguia, A.; Stradigl, C.; Alkhraisat, M.H. Clinical performance of additively manufactured subperiosteal implants: A systematic review. *Int. J. Implant Dent.* 2024, **10** (1), 4.
17. Kundakcioglu, A.; Ayhan, M. Evaluation of different subperiosteal implant thicknesses on mechanical strength and stress on bone by finite element analysis. *Int. J. Med. Sci.* 2024, **21** (9), 1672-1680.
18. Keleş, H.G.; Karaca, Ç. Comparison of stress distribution among standard dental implants placed in grafted bone, zygomatic implants, and subperiosteal implants in the atrophic edentulous maxilla: 3D finite element analysis. *Int. J. Oral Maxillofac. Implants* 2023, **38** (2), 347-356.
19. Cawood, J.I.; Howell, R.A. A classification of the edentulous jaws. *Int. J. Oral Maxillofac. Surg.* 1988, **17** (4), 232-236.
20. De Moore, E.; Huys, S.E.F.; Vn Lenthe, D.H.; Mommaerts, M.Y.; Sloten, J.V. Mechanical evaluation of a patient-specific additively manufactured subperiosteal jaw implant (AMSJI) using finite-element analysis. *Int. J. Oral Maxillofac. Surg.* 2022, **51** (3), 405-411.
21. Miyamoto, S.; Ujigawa, K.; Kizu, Y.; Tonogi, M.; Yamane, G.Y. Biomechanical three-dimensional finite-element analysis of maxillary prostheses with implants: Design of number and position of implants for maxillary prostheses after hemimaxillectomy. *Int. J. Oral Maxillofac.* 2010, **39**, 1120-1126.
22. Ayhan, M.; Cankaya, A.B. Custom-made subperiosteal implants: A finite element analysis on monoblock and dual implant systems in atrophic maxilla. *Int. J. Med. Sci.* 2023, **20** (13), 1755-1762.
23. Antiparmak, N.; Polat, S.; Onal, S. Finite element analysis of the biomechanical effects of titanium and Cfr-peek additively manufactured subperiosteal jaw implant (AMSJI) on maxilla. *J. Stomatol. Oral Maxillofac. Surg.* 2023, **124** (1S), 101290.
24. Zielinski, R.; Sowinski, J.; Piechaczek, M.; Okulski, J.; Kozakiewicz, M. Finite element analysis of subperiosteal implants in edentulism - on the basis of the Mai Implant® by Integra Implants®. *Materials (Basel)* 2023, **16** (23), 7466.
25. Liao, X.; Cao, R.; Zhong, J.; Chen, C.; Pan, S. Influence of implant distribution on the biomechanical behaviors of mandibular implant-retained overdentures: A three-dimensional finite element analysis. *Int. J. Med. Sci.* 2024, **24** (1), 405.

Disclaimer/Publisher's Note: The statements, opinions and data contained in all publications are solely those of the individual author(s) and contributor(s) and not of MDPI and/or the editor(s). MDPI and/or the editor(s) disclaim responsibility for any injury to people or property resulting from any ideas, methods, instructions or products referred to in the content.